NANO LETTERS

Letter

pubs.acs.org/NanoLett

Semiconductor Nanorod–Carbon Nanotube Biomimetic Films for Wire-Free Photostimulation of Blind Retinas

Lilach Bareket,[†,‡] Nir Waiskopf,[§,∥] David Rand,[†,‡] Gur Lubin,[†,‡] Moshe David-Pur,[†,‡] Jacob Ben-Dov,[†,‡] Soumyendu Roy,[†,‡] Cyril Eleftheriou,[#] Evelyne Sernagor,[#] Ori Cheshnovsky,[⊥,‡] Uri Banin,[§,∥] and Yael Hanein*[,†,‡]

[†]School of Electrical Engineering, [‡]Tel Aviv University Center for Nanoscience and Nanotechnology, and [⊥]School of Chemistry, Tel Aviv University, Tel Aviv 69978, Israel

[§]Institute of Chemistry and [∥]Center for Nanoscience and Nanotechnology, The Hebrew University of Jerusalem, Jerusalem 91904, Israel

[#]Institute of Neuroscience, Faculty of Medical Sciences, Newcastle University, Newcastle upon Tyne, NE2 4HH, United Kingdom

Supporting Information

ABSTRACT: We report the development of a semiconductor nanorod-carbon nanotube based platform for wire-free, light induced retina stimulation. A plasma polymerized acrylic acid midlayer was used to achieve covalent conjugation of semiconductor nanorods directly onto neuro-adhesive, three-dimensional carbon nanotube surfaces. Photocurrent, photovoltage, and fluorescence lifetime measurements validate efficient charge transfer between the nanorods and the carbon nanotube films. Successful stimulation of a light-insensitive chick retina suggests the potential use of this novel platform in future artificial retina applications.

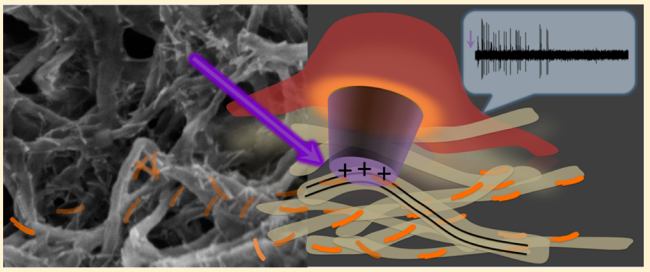

KEYWORDS: *Neural photostimulation, carbon nanotubes, quantum rods, retinal implant, neural prosthesis, plasma polymerization*

A wide range of medical conditions is associated with dysfunctional neuronal connectivity and sensory information transfer to the brain. Neuroprosthetic systems attempt to treat these conditions, and several devices are already in medical use to treat deafness, Parkinson's disease, and chronic pain, to name just a few.[1−3] Visual prosthetic devices are presently developed as an approach to treat blindness. In particular, there is a dire need to help the ever growing number of patients suffering from age-related macular degeneration in which the photoreceptors in the retina degenerate. A particular challenge is the need for high-resolution stimulation, along with effective interfacing with the remaining neurons in the retina. Contemporary approaches to address these challenges are based on metallic electrodes and are typified by relatively low spatial resolution, rigidity, and cumbersome wiring.[4,5] Neuronal activation with optical stimulation of photoresponsive surfaces[6] offers an alternative, wire-free route to address the need for artificial vision.[7−9] Several approaches have been recently proposed including conducting polymers (CPs)[10−12] and quantum dot (QD) films.[13−15] QDs directly interfacing the cell membrane were also suggested.[16] Recent studies employing CPs as a photoactive layer have attracted considerable attention as they offer advantages such as simple fabrication and mechanical flexibility.[17] The major disadvantages of CPs are their low stability under continuous stimulation, exposure to ultraviolet (UV) light or heat which may gradually degrade their properties,[18,19] as well as the risk of toxic residues. These issues have yet to be tested to fully explore the potential of these materials in retinal implant applications.

An additional emerging approach to vision restoration is optogenetics, most commonly including the introduction of bacterial opsins into neurons through viral transfection.[20] Recent studies have demonstrated the use of optogentics for restoring light-sensitivity to residual cells in a degenerate retina.[21,22] The optogenetics approach offers high temporal resolution and cell specificity, and it is minimally invasive. Nevertheless, there are still many challenges that have to be overcome to make this technology suitable for application in vision restoration. Foremost is the long-term expression of light sensitive proteins to avoid the need for repeated injections, controlling and sustaining gene expression and the efficiency of transfection methods. Semiconductor nanocrystal (SCNC) systems are particularly attractive for neuronal stimulation applications due to their tunable optical and electronic properties, photostability, and chemical interfacing diversity. However, despite extensive efforts, efficient SCNC mediated neuronal stimulation with ambient light intensities has not been demonstrated yet. Here, we introduce a novel approach for

Received: September 7, 2014
Revised: October 25, 2014
Published: October 28, 2014

   dx.doi.org/10.1021/nl5034304 | *Nano Lett.* 2014, 14, 6685−6692

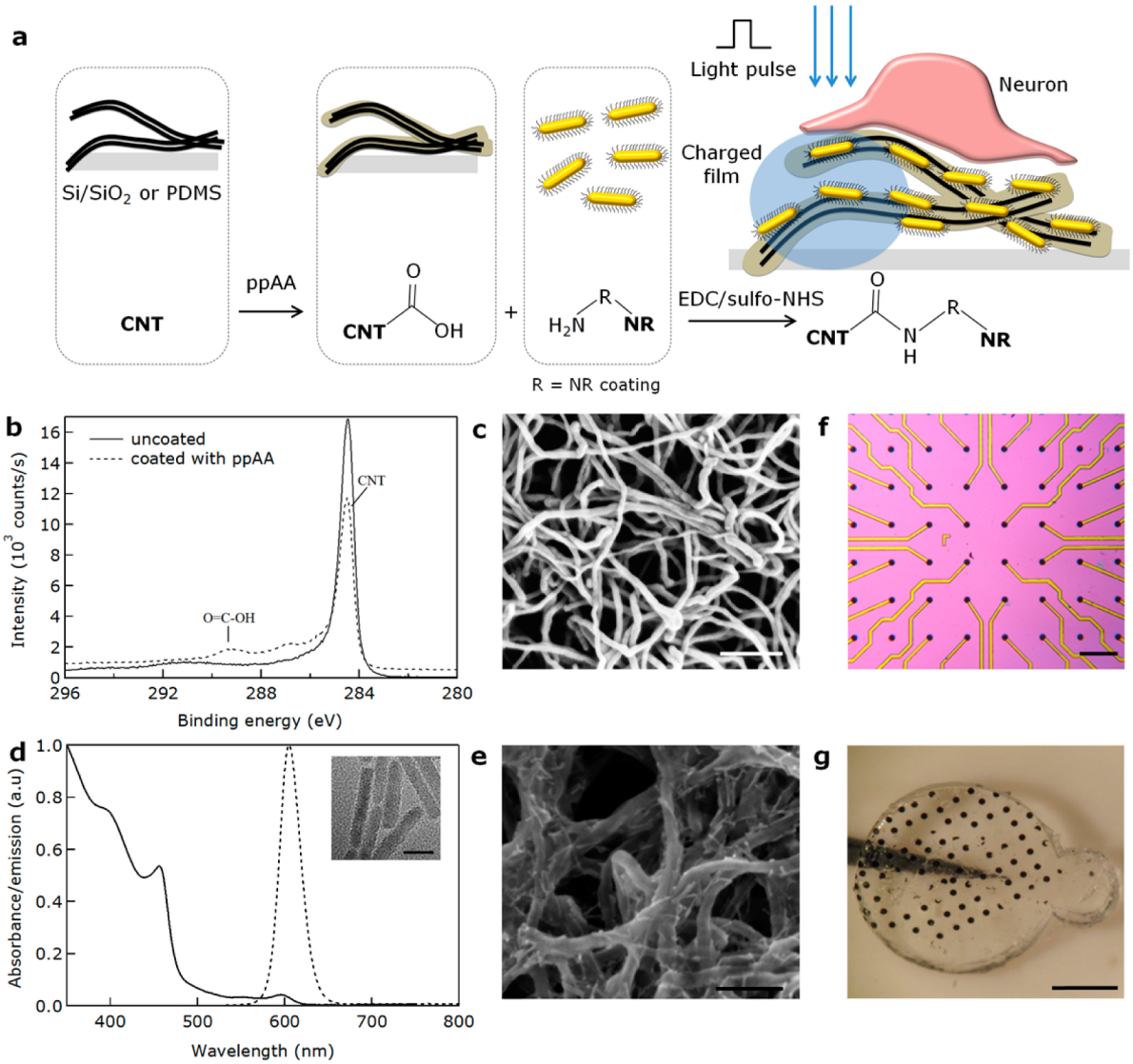

Figure 1. NR−CNT films and electrode arrays. (a) Schematic representation of the photoactive electrode preparation. NR conjugation onto a CNT film is based on covalent binding enabled by a ppAA coating of the CNTs. Light is absorbed by the film, followed by charge separation at the NR−CNT interface which elicits a neuronal response. (b) XPS chemical analysis of pristine (continuous line) and ppAA coated CNT film (dashed line) demonstrating the formation of carboxylic groups. (c) SEM image of a ppAA coated CNT film demonstrating preservation of porous structure; the scale bar is 200 nm. (d) Absorption (continuous line) and emission (dashed line) spectrum of the CdSe/CdS NRs; Inset: a TEM image of the CdSe/CdS NRs; the scale bar is 20 nm. (e) SEM image of a NR−CNT film; the scale bar is 100 nm. NRs appear as bright elongated elements on the CNTs. (f) An optical microscope image of a CNT multi electrode array (MEA); the scale bar is 200 μm. (g) CNT electrode array on a PDMS flexible support; the scale bar is 1 mm.

wire-free retinal photostimulation, based on a combination of two nanomaterial systems ideally suited for neurostimulation: semiconductor nanorods (NRs) and carbon nanotubes (CNTs) (Figure 1a). The nanorod geometry enables efficient light absorbance, followed by effective charge separation at the NR−CNT interface.[23] CNTs are particularly suitable for this application having superior neuronal recording and stimulation properties[24,25] originating from their high surface roughness[26,27] and biomimetic nature.[28,29] The use of highly porous three-dimensional CNTs as SCNC carrying microelectrodes therefore supports high SCNC loading along with the formation of an electrochemically safe interface, with excellent coupling with the neuronal tissue.[30]

To achieve clean and effective NR−CNT conjugation, we developed a special covalent bonding scheme based on plasma-polymerized acrylic acid (ppAA) coated CNT films, amine modified NRs, and carbodiimide chemistry (Figure 1a). High-density CNT films were first grown on titanium nitride (TiN) coated silicon/silicon dioxide (Si/SiO_2) substrates using chemical vapor deposition (CVD) which supports CNT patterning, film porosity, and cleanliness. CNT films were then coated with a ppAA coating featuring carboxylic functional groups (needed for the conjugation step) using a plasma polymerization process. The plasma polymerization offers high conformity, strong adhesion, and surfaces containing no contaminates.[31,32] X-ray photoelectron spectroscopy (XPS) data of the ppAA coated CNT films show a clear carboxylic group (O═C−OH) peak component, which is absent in pristine CNT films, validating the buildup of a ppAA (Figure 1b).

Scanning electron microscopy (SEM) imaging of the CNT surface after plasma polymerization reveals that the CNT films

dx.doi.org/10.1021/nl5034304 | Nano Lett. 2014, 14, 6685−6692

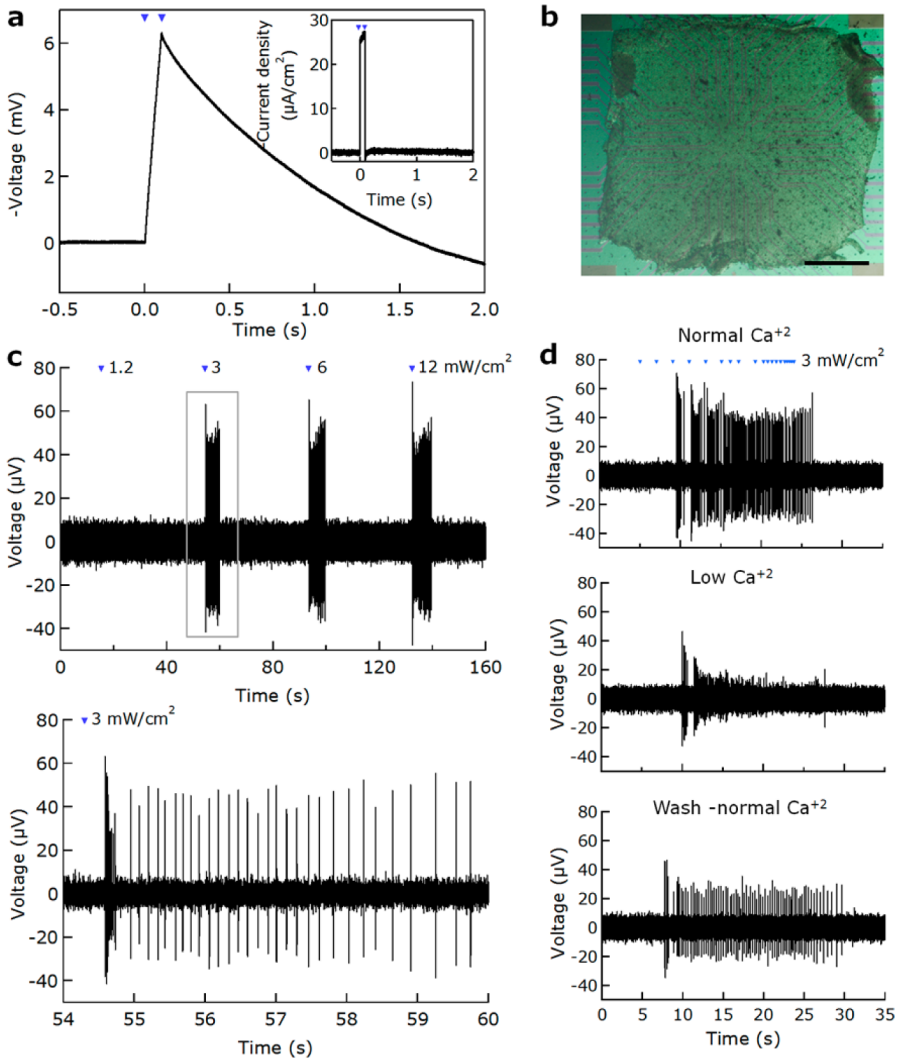

Figure 2. Embryonic chick retina stimulation with NR−CNT electrodes. (a) Photovoltage (negative polarity) of a CdSe/CdS−GSH NR−CNT electrode versus time (electrode diameter 210 μm). Electrodes were illuminated with a violet light source (405 nm) for 100 ms at intensity of 70 mW/cm^2. Inset: Photocurrent versus time for the same electrode under the same illumination conditions. (b) A chick retina (E14) placed on a CdSe/CdS−GSH NR−CNT MEA; the scale bar is 500 μm. (c) Extracellular voltage trace (top) recorded from a chick retina following 100 ms light stimulation (405 nm; pulse interval of 30 ms) at different intensities (1.2, 3, 6, and 12 mW/cm^2; stimulation pulses are marked by blue arrow heads). The bottom panel is an enlargement of the spike burst following a light pulse of 3 mW/cm^2. (d) Extracellular voltage traces recorded from a chick retina under illumination with 3 mW/cm^2 and 30 ms pulses (405 nm; marked by blue arrow heads) with different interpulse intervals (2 s, 1 s, 500 ms, 250 ms; repeated five times for each interval) when maintained in a control medium (2.5 mM Ca^{2+}; top), low Ca^{2+} medium (0.5 mM Ca^{2+}; middle), and measured again in a medium with normal Ca^{2+} concentration (2.5 mM Ca^{2+}; bottom).

retained their porous and entangled surface (Figure 1c). This high porosity is important to maintain the CNT's superior electrochemical features and their adhesiveness to neuronal tissue.[25,30]

Prototypical cadmium selenide/cadmium sulfide (CdSe/CdS; core/shell) NRs were used as a model system for SCNCs. NRs were synthesized in a seeded growth approach using a modification of a previously described synthesis procedure.[33] Figure 1d shows the absorption and emission spectra and a transmission electron microscopy (TEM) image of these NRs. The absorption spectrum (continuous line) manifests a weak first exciton peak at 600 nm related to the CdSe seed and a sharp increase in absorption below 470 nm mainly due to the contribution of the CdS shell. The emission spectrum (dashed line) shows a peak at 610 nm. TEM imaging of these CdSe/CdS NRs reveals a homogeneous size distribution, 40 ± 5 nm in length and 5 ± 0.8 nm in diameter (Figure 1d, inset).

To render the NRs soluble in an aqueous solution and to support their conjugation with the CNT films, organic ligands from the synthesis stage were replaced with the antioxidant, tripeptide−glutathione (GSH), using a ligand exchange process.[34] The GSH coating also helps in stabilizing and protecting the SCNCs as will be elaborated later in the text. GSH coated CdSe/CdS NRs (CdSe/CdS−GSH NRs) were covalently conjugated to the ppAA coated CNT film using carbodiimide chemistry[35] with 1-(3-(dimethylamino)propyl)-3-ethylcarbodiimide hydrochloride (EDC) and *N*-hydroxysulfosuccinimide (sulfo-NHS). SEM imaging validates effective NRs conjugation across the CNT surface without NR aggregation (Figure 1e), as well as NR penetration into the three-dimensional CNT matrix (see Figure S1). Having established a successful loading of NRs onto CNT/ppAA film, this

dx.doi.org/10.1021/nl5034304 | *Nano Lett.* 2014, 14, 6685−6692

approach was used to deposit SCNCs on patterned CNT/ppAA multielectrode arrays (CNT MEAs) (Figure 1f). Moreover, patterned CNT/ppAA/NR electrodes can be transferred onto a flexible support such as poly-(dimethylsiloxane) (PDMS) for implantation purposes (Figure 1g).[36] CNT MEA fabrication process is described at length in Gabay et al. (2007)[24] and CNT pattern transfer to PDMS films in David-Pur et al. (2014).[37]

To validate the effectiveness of the NR−CNT film for optical stimulation of a light-insensitive neuronal tissue, photovoltage and photocurrent measurements were conducted using a modulated light source. CdSe/CdS−GSH NR−CNT electrodes (210 μm in diameter) were immersed in phosphate buffered saline (PBS). Open-circuit voltage (Figure 2a) and short-circuit current (Figure 2a, inset) were measured using a high surface area platinum mesh as a reference electrode. Photovoltage traces (Figure 2a) are typified by a voltage increase during illumination (to negative values), followed by a discharge when light is turned off. Such characteristics can be explained by an equivalent simplified circuit consisting of a current source and a diode coupled with the electrochemical interface of the CNT system (see Figure S2a). The rate of charging−discharging of a capacitor through passive and resistive circuit elements is inversely proportional to the electrochemical electrode capacitance. Since CNT films have a large surface area, they also have a large capacitance at the CNT−electrolyte interface. During illumination the electrons generated by photoexcitation accumulate at this capacitor. After light is turned off, the capacitor discharges slowly, and hence the recorded voltage also drops slowly.

Light-insensitive embryonic chick retinas at day 14 of development (E14) were used as a neuronal model. Waves of spontaneous activity originating from retinal ganglion cells (RGCs) at E13−18,[38] and the acquirement of photosensitivity by photoreceptors as well as by intrinsically photosensitive retinal ganglion cells (ipRGCs; the melanopsin dependent non-image-forming pathway) typifies the development of these retinas. At E14, retinal cells are at early maturation stage, and photoreceptors are not yet developed. The mRNA of the long wave cone opsins only begins to appear at E14, and transcripts of rhodopsin and of short waves cones opsins begin to appear at E15.[39] Photoreceptor electrical activity in response to light is not detected before E17.[40] Although melanopsin expression starts as early as E4,[41] ipRGCs are less sensitive to light than photoreceptors and require light stimulation of several seconds to evoke a response.[42] We have validated the light insensitivity of our neuronal model by demonstrating that photostimulation of E14 retinas (n = 19), placed on commercial TiN MEA (MultiChannel Systems), did not elicit neuronal activity[12] (see also Figure S3a). Retinas (n = 4) were placed on CdSe/CdS−GSH NR−CNT MEAs, which were used for both optical stimulation and simultaneous electrical recording, with the RGC layer facing down (Figure 2b). Extracellular electrical signals of retina activity were recorded following pulsed photostimulation using different pulse durations and intensities of violet light (405 nm).

The data in Figure 2c and d show a pronounced electrical response to 100 ms photostimulation. Excitation intensities were varied within the range of 1.2−12 mW/cm^2 (Figure 2c, top) (corresponding with ambient light intensities), revealing an intensity threshold of 3 mW/cm^2. Repetitive pulses of subthreshold stimulus (30 ms at 3 mW/cm^2) resulted in a delayed response (Figure 2d, top), indicating a charge buildup in the NR−CNT interface owing to the slow discharge kinetics.

A closer inspection of the data reveals two time scales (Figure 2c, bottom): A short latency burst with rapid activity and a long latency response typified by a tonic spiking activity. This time separation is conspicuously similar to the separation observed in conventional electrical stimulation where direct (RGC) and indirect (bipolar cell) activations are typically discernible.[43] The presence of axon collaterals projecting back to the inner plexiform layer in embryonic chick retina may also be responsible for these late responses.[44] Owing to the low current generated by the NR−CNT electrodes, the typical stimulation times are long, yielding markedly longer latency values than commonly obtained in electrical stimulation (~1 ms) for direct response. Moreover, while direct activation is highly synchronized in electrical stimulation, here it appears sparse with little overlap between different activated elements. This effect is likely a direct result of the slow activation, causing different elements to respond at different times. The biological nature of this light induced electrical activation of the retina was further revealed using a low calcium (Ca^{2+}) medium (using 0.5 mM of $CaCl_2$ and additional 2 mM of $MgCl_2$), in which synaptic activity is hampered (Figure 2d). Under these conditions, the long latency response is markedly reduced, indicating the synaptic nature of the indirect response, while the short latency and rapid response remains intact.

Retinas were left on the NR−CNT MEAs for as long as 24 h and retained their spontaneous activity, validating their physiological viability on these surfaces (see also Figure S3c). Additionally, a cell viability assay was conducted, testing the viability of primary neurons cultured on CdSe/CdS−GSH NR−CNT patterns compared with neurons cultured on poly-D-lysine coating (a standard culturing environment for embryonic rat neurons). Cell viability was monitored at 7, 14, and 21 days in vitro. No significant differences were found in cell viability under normal culturing conditions (see Figure S4).

The CdSe/CdS−GSH NR deposition protocol described above is the obtained optimum after experimenting with several alternative materials and procedures. Various conjugation procedures and SCNC configurations were systematically explored to better understand the underlying principles until highly efficient surfaces were realized. Three different particle architectures were compared: CdSe QDs with a diameter of 3.7 ± 0.1 nm, CdSe/CdS QDs with a diameter of 7 ± 0.8 nm, and CdSe/CdS NRs with a diameter of 5 ± 0.8 nm and length of 40 ± 5 nm (Figure 3a), all coated with GSH (CdSe−GSH, CdSe/CdS−GSH, and CdSe/CdS NR−GSH; see also Figure S5 for SCNC optical characterization). First, the particle loading, derived from inductively coupled plasma mass spectrometry (ICP-MS) analysis, was investigated.

The amount of CdSe−GSH QDs deposited on the CNT films was found to be, on average ~10^{14} particles/cm^2, an order of magnitude larger than CdSe/CdS−GSH QDs and CdSe/CdS−GSH NRs with ~10^{13} particles/cm^2 (Figure 3b, top). As CdSe−GSH QDs are smaller, compared with the CdSe/CdS−GSH QDs, this effect may be attributed to the size of the SCNCs. It is also important to note that, to accommodate good solubility, the maximum concentrations achievable without discernible SCNC aggregation were used (300−900 nM, 100 nM, and 20−40 nM for CdSe−GSH QDs, CdSe/CdS−GSH QDs, and CdSe/CdS−GSH NRs, respectively).

Loading efficiency provides important information, yet it does not reveal whether the loaded SCNC contribute to

dx.doi.org/10.1021/nl5034304 | Nano Lett. 2014, 14, 6685−6692

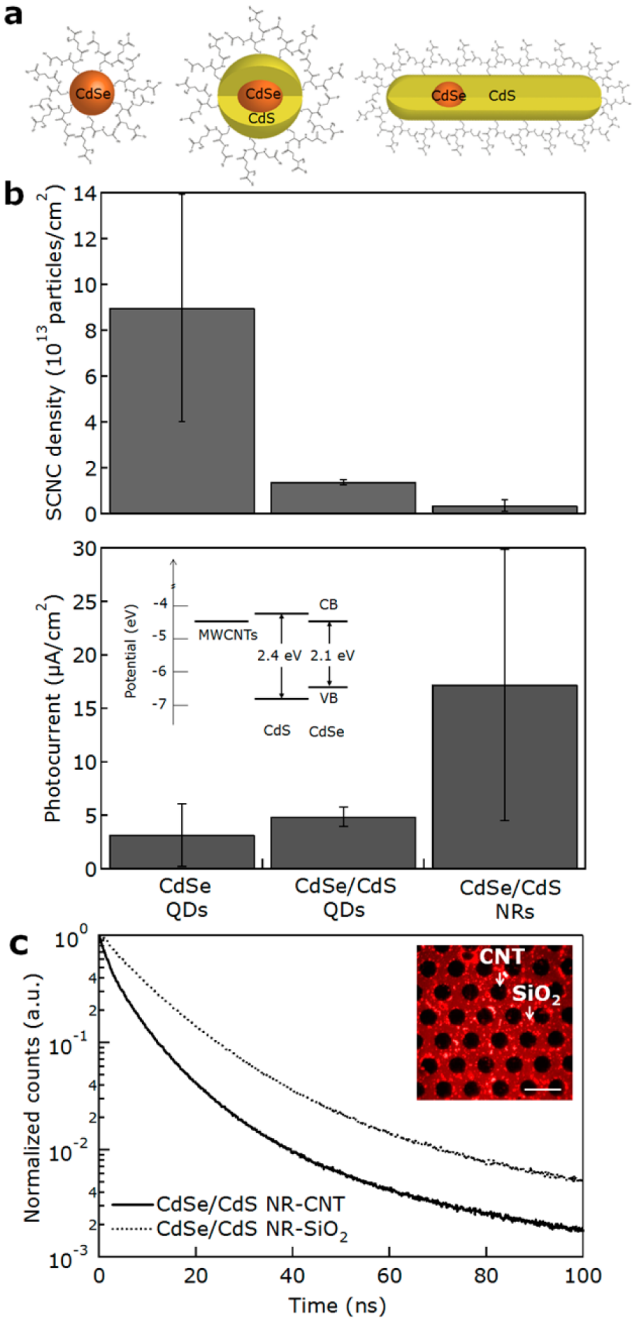

Figure 3. SCNC loading on CNT films. (a) Schematic drawing of the SCNCs compared: CdSe–GSH QDs (left), CdSe/CdS–GSH QDs (center), and CdSe/CdS–GSH NRs (right). (b) Loading yield derived from ICP-MS analysis of different SCNCs (top). Average photocurrent for different SCNCs recorded following an excitation pulse of 30 mW/cm^2 for 100 ms with a 405 nm illumination source (bottom). Highest photocurrents were obtained with CdSe/CdS–GSH NRs. Inset: A schematic band diagram of the CdSe/CdS NR–CNT system. (c) Photoluminescence lifetime data of CdSe/CdS–GSH NR conjugated to CNTs (solid line) and to SiO_2 (dotted line). Inset: Fluorescence microscope image of CNT pattern on SiO_2 substrate. CNTs and SiO_2 substrate are coated with CdSe/CdS-GSH NRs; the scale bar is 200 μm.

efficient charging of the interface. Poor charge transfer may be associated with SCNC intrinsic properties such as the number of surface traps and volume, or system properties such as the formation of SCNC aggregates, poor SCNC–CNT coupling, and differences in band offsets between the SCNCs and the CNTs, which hinder light induced charge transfer. To investigate which of the films described above yielded good electrical properties, photocurrent measurements of coated CNT films (0.46 cm^2, defined by illumination spot size) were measured. Peak photocurrent values were extracted for each sample from the photocurrent traces (measured at 30 mW/cm^2; see also Figure S2). As can be seen in Figure 3b, while CdSe–GSH QDs were effectively deposited on the CNT films, they yielded poor photocurrent values. The best photocurrent values were obtained with CdSe/CdS–GSH NRs. The band diagram describing CdSe/CdS NR–CNT interface presented in the inset of Figure 3b supports a mechanism of electron transfer from the excited NRs to the CNTs. Based on these results, CdSe/CdS–GSH NR were chosen as the CNT coating material for retina stimulation.

The spectral response of the CdSe/CdS–GSH NR–CNT films 530, 660, and 850 nm shows almost no photocurrent (see Figure S2b). This result is consistent with the NR absorption spectrum (Figure 1d), confirming the role of the NRs in facilitating light induced charge separation at the NR–CNT interface. Furthermore, the spectral sensitivity demonstrates the tunability of the system, which may be exploited for future development of color selective films. We note the increase in photocurrent with increased intensity (Figure S2c) and the reliability of the photocurrent response with repetitive stimulations (Figure S2c, inset). Additionally, we validated that the covalent conjugation contributes to improved photocurrent compared with physical adsorption (see Figure S6, bottom).

Finally, we compared fluorescence lifetime measurements of dry CdSe/CdS–GSH NR–CNT films to results from CdSe/CdS–GSH NRs deposited on SiO_2 (CdSe/CdS–GSH NR–SiO_2) (Figure 3c). It is clearly apparent that the proximity of the CNTs shortens the CdSe/CdS–GSH NR fluorescence lifetime, consistent with charge separation at the NR–CNT interface introducing a competing mechanism to the fluorescent recombination of charge carriers. These findings are further supported by previous studies demonstrating light induced charge transfer between QDs and CNTs.[45,46] Moreover, in fluorescence imaging of patterned CNT films on SiO_2 substrate, with NRs conjugated to the surface (Figure 3c, inset), NR–CNT regions appear dark compared to the fluorescence of the NR–SiO_2 background. This effect is consistent with the existence of a charge transfer from the CdSe/CdS–GSH NRs to the CNTs. Fully understanding the underlying mechanisms of light harvesting, charge separation, and photocurrent generation in our novel nanostructured device remains a challenge, under ongoing study in our laboratories.

Indeed, to fit in vivo applications, the system must retain its inertness and its performance without causing toxic effects. SCNCs, especially free in solution, may induce adverse cytotoxicity effects[47,48] originating from their toxic composition and from their nanoscale size.[49] The most predominant cause for SCNC cytotoxicity is the generation of reactive oxygen species and/or release of cadmium ions to the solution upon photoexcitation.[49,50] These may interact with proteins or DNA, leading to mutations and cell death. The retina stimulation experiments presented here validated the short-term biocompatibility (up to 24 h) of these systems (see also Figure S3). Long-term in vitro stability (up to 21 days) was validated using viability tests of dissociated cortical neurons (as described earlier in this text; see also Figure S4). It is important to note

dx.doi.org/10.1021/nl5034304 | Nano Lett. 2014, 14, 6685–6692

that the coating material plays a crucial role in stabilizing and protecting SCNC from degradation and is therefore an important parameter in determining the safety and stability of the CdSe/CdS NR−CNT system. GSH is a well-known natural antioxidant molecule that can contribute also to an improved biocompatibility.[51] Our investigation has indeed validated the in vitro biocompatibility of these systems. Further optimization of the stability of the system toward implementation in long-term in vivo applications will be needed and is beyond the scope of this investigation. By effectively incorporating SCNCs onto CNT surfaces, highly efficient photoresponsive porous films were realized, demonstrating for the first time a nanomaterial based approach for retinal photostimulation with better performances and a path toward further optimization.

Most notably, not only our nano interfaces provide highly efficient photosensitivity, but equally important, they form a truly three-dimensional interface with optimized binding between the biological tissue and the optoelectronic device.[27,30] The use of a three-dimensional matrix as well as an optimized selection of SCNCs, their surface coating, and conjugation procedure contributes to the superior properties of these films. Several pioneering studies reported the use of QDs and CPs to elicit a neuronal response. In the only report to date to achieve neuronal activation with QDs, a 800 mW/cm^2 intensity was used[15] (compared with 3 mW/cm^2 reported here). Membrane hyperpolarization or depolarization was achieved using an intensity of ∼0.36 mW/cm^2.[13] Polymeric systems have achieved stimulation with values ranging from 0.03 to 1500 mW/cm^2.[10−12] The lowest value was achieved in a subretinal configuration using a retina with residual light sensitivity, making the exact comparison to our system cumbersome. Compared with previously reported neural photostimulation technologies utilizing CPs and QDs, our CNT−NR interfaces have an improved efficiency (i.e., lower threshold for evoking action potentials), durability, flexibility, and the demonstrated capacity to elicit localized stimulation. The stable CNT interface, with its capacitive charge transfer mechanism and low impedance, is overall an optimal platform for efficient neuronal light induced stimulation.[24,37] NRs embedded onto CNT films offer several advantages compared with a photoconductive semiconductor substrate. Silicon devices developed for artificial vision are rigid and inherently nontransparent, necessitating a complicated implantation procedure and an external power source. Polymeric based systems, which are emerging as an alternative for silicon, will have to overcome long-term stability issues typifying such systems. Both silicon and polymeric based solution do not offer the special tissue binding properties of CNTs. Furthermore, compared with utilizing an injected SCNC system our NR−CNT platform contributes to increased charge separation, as demonstrated by fluorescence lifetime results (see Figure 3c), and helps anchoring the SCNC to a substrate thus preventing them from uncontrolled and possible harmful migration in the tissue. The use of a bottom up approach implies that the technology can be further improved, owing to massive activity in this field. The CdSe/CdS−GSH NR−CNT photoresponsive electrodes presented here represent a major step toward achieving a wire-free retinal prosthesis and a paradigm shift from two-dimensional to significantly superior three-dimensional biomimetic opto-electrical interfacing.

Experimental Section. *SCNC Preparation and Coating.* CdSe QDs were synthesized by fast injection of selenium dissolved in trioctylphosphine (TOP) solution into a four-necked flask containing cadmium oxide (CdO) in trioctylphosphine oxide (TOPO) and *n*-octadecylphosphonic acid (ODPA) at 350 °C under argon atmosphere. The crude solution was then washed with methanol to remove excess ligands. CdSe/CdS QDs and NRs were synthesized following previously described protocols based on a seeded growth approach.[52] CdSe SCNCs were mixed with elemental sulfur dissolved in TOP. This solution was rapidly injected into a four-neck flask containing TOPO, ODPA, and CdO for the synthesis of CdSe/CdS QDs, or TOPO, ODPA, CdO, and hexylphosphonic acid (HPA) for the synthesis of the CdSe/CdS NRs at 360 °C. After cooling, the crude solution was dissolved in toluene, and methanol was added in order to precipitate the NCs and remove excess precursors and ligands. GSH coating was used to render SCNCs with amine functionality and soluble in an aqueous solution. The SCNC surface coating was modified using previously described process.[53] 200 μL of a GSH solution containing of 0.459 mmol of GSH and 100 mg of potassium hydroxide in 1 mL of methanol were mixed with 1 mL of SCNCs in chloroform. Basic triple-distilled water (TDW) (2 mL, pH 11−12) was added, and a water phase containing SCNCs coated with GSH was obtained. After phase transfer, an excess of ligands or polymer were washed by filtration using 100 kDa cellulose membrane filters (Invitrogen Corp.).

Conjugating SCNCs to High-Density CNT Patterns. CNT films were then coated with acrylic acid (Sigma-Aldrich) by plasma polymerization (Pico-RF, Diener) using an input power of 40 W and acrylic acid vapor pressure of 0.2 mbar for 2 min. ppAA-coated CNTs were then incubated in a solution of 0.1 M EDC (Sigma-Aldrich) and 5 mM sulfo-NHS (PIERCE) in PBS for 30 min at room temperature. Following the 30 min activation, samples were washed with deionized water (DI), and SCNCs were added. The CNT substrate and SCNC solution were then incubated at 50 °C overnight. Finally, samples were washed three times with DI.

XPS measurements were performed using a 5600 Multi-Technique System (Physical Electronics).

Structural characterization of CdSe/CdS−GSH NR−CNT films was performed using SEM (MagellanTM 400L) and TEM (Tecnai G^2 Spirit Twin T-12).

SCNC Optical Characterization. Absorbance spectra were measured using a UV−vis−near−IR spectrophotometer (JASCO V-570). Photoluminescence spectra were measured using a fluorimeter (Varian Inc.), and fluorescence lifetime measurements were carried out using a fluorescence spectrometer (Edinburgh Instruments FLS920).

ICP-MS Measurements. For ICP-MS, patterns of 0.5 cm × 0.5 cm CNT films, loosely attached to the Si/SiO$_2$ substrate, were conjugated with SCNCs. CNT−SCNCs were peeled off the substrate and etched overnight in 1 mL of 69% nitric acid. Following sonication, 100 μL of the CNT−SCNCs solution was mixed with 3.35 mL of TDW and analyzed by ICP-MS (cx7500, Agilent) for Cd. The quantity of Cd in each solution was calculated using external calibration with standard Cd solutions.

Photoresponse. The illumination unit consisted of a light-emitting diode (LED) with a peak wavelength of 405 nm (Thorlabs) mounted on an upright metallurgical microscope (Meiji), using a 4× or a 40× water immersion objective, resulting in illumination intensities within the range of 0.6−70 mW/cm^2. LEDs with a peak wavelength at 530, 660, and 850 nm (Thorlabs) were used to study spectral response. The

dx.doi.org/10.1021/nl5034304 | Nano Lett. 2014, 14, 6685−6692

measurement unit consisted of a current amplifier (model 1212; DL Instruments) or voltage amplifier (model 1800; A-M Systems). A photogenerated current or voltage was measured between the illuminated electrode and a reference electrode (platinum mesh) in PBS.

Electrical Recordings from Retinas. Coupling between the tissue and the electrodes was improved by placing a small piece of polyester membrane filter (5 μm pores; Sterlitech) and a ring weight on the retina. The filter was removed before light stimulation to minimize scattering. Retinas were kept at physiological conditions,[54] at a temperature of 34 °C, and perfused (2−5 mL/min) with oxygenated (95% O_2, 5% CO_2) Tyrode's solution (5 mM KCl, 25 mM $NaHCO_3$, 9 mM glucose, 1.2 mM $MgSO_4$, 1.2 mM HEPES, 0.5 mM glutamine, 2.5 mM $CaCl_2$). Neuronal signals were amplified (gain ×1200 MEA1060-Inv; MultiChannel Systems), digitized using a 64-channel analogue to digital converter (MC_Card; MultiChannel Systems), and recorded (MC_Rack; MultiChannel Systems).

■ ASSOCIATED CONTENT

Supporting Information

Figure S1 showing cross section SEM imaging of CdSe/CdS−GSH NR−CNT film, Figure S2 showing photocurrent characterization and electrical circuit model of CdSe/CdS−GSH NR−CNT films, Figure S3 showing chick retina spontaneous activity and photostimulation, Figure S4 showing in vitro cell viability assay results, Figure S5 showing optical properties of SCNCs used, and Figure S6 showing loading yield of and average photocurrent of CdSe/CdS−GSH NR−CNT films using covalent conjugation and physical adsorption. This material is available free of charge via the Internet at http://pubs.acs.org.

■ AUTHOR INFORMATION

Corresponding Author

*E-mail: yaelha@tauex.tau.ac.il.

Author Contributions

L.B., N.W., and D.R. contributed equally to this work. L.B., N.W., D.R., Y.H., U.B., and O.C. conceived and designed the experiments. L.B., N.W., D.R., G.L., M.D.P., and J.B.D. performed the experiments and analysis. E.S and C.E. advised with retina experiments. S.R. helped with electrical modeling. L.B. and Y.H. wrote the manuscript, and all authors reviewed and discussed it. Y.H., U.B., and O.C. supervised the project.

Notes

The authors declare no competing financial interest.

■ ACKNOWLEDGMENTS

The authors thank Larisa Burstein for XPS measurements, Inna Brainis and Gilad Cohen for assistance with the neuronal cell cultures, Qlight Nanotech for some of the SCNCs, and Shlomo Yitzhaik for many useful discussions. The work described in this paper was partially supported by a grant from the Israel Ministry of Science and Technology (O.C., U.B., and Y.H.), by a grant from the European Research Council funding under the European Community's Seventh Framework Program (FP7/2007−2013)/ERC grant agreement FUNMANIA-306707 (Y.H.) and by a grant from the Biotechnology and Biological Sciences Research Council (BBSRC BB/1023526/1) (E.S.). U.B. thanks the Alfred & Erica Larisch memorial chair. N.W. was supported by a Clara Robert Einstein Scholarship.

■ REFERENCES

(1) Clark, G. M. *Philos. Trans. R. Soc. B* **2006**, *361*, 791−810.
(2) Plow, E. B.; Pascual-Leone, A.; Machado, A. *J. Pain* **2012**, *13*, 411−424.
(3) Wichmann, T.; DeLong, M. R. *Neuron* **2006**, *52*, 197−204.
(4) Cogan, S. F. Neural stimulation and recording electrodes. In *Annu. Rev. Biomed. Eng.*, **2008**; Vol. *10*, pp 275−309.
(5) McConnell, G. C.; Rees, H. D.; Levey, A. I.; Gutekunst, C. A.; Gross, R. E.; Bellamkonda, R. V. *J. Neural Eng.* **2009**, *6*, 1−12.
(6) Bareket-Keren, L.; Hanein, Y. *Int. J. Nanomed.* **2014**, *9*, 65−83.
(7) Chow, A. Y.; Chow, V. Y.; Packo, K. H.; Pollack, J. S.; Peyman, G. A.; Schuchard, R. *Arch. Ophthalmol.* **2004**, *122*, 460−469.
(8) Zrenner, E.; Bartz-Schmidt, K. U.; Benav, H.; Besch, D.; Bruckmann, A.; Gabel, V. P.; Gekeler, F.; Greppmaier, U.; Harscher, A.; Kibbel, S.; Koch, J.; Kusnyerik, A.; Peters, T.; Stingl, K.; Sachs, H.; Stett, A.; Szurman, P.; Wilhelm, B.; Wilke, R. *Proc. R. Soc. B* **2011**, *278*, 1489−1497.
(9) Wang, L. L.; Mathieson, K.; Kamins, T. I.; Loudin, J. D.; Galambos, L.; Goetz, G.; Sher, A.; Mandel, Y.; Huie, P.; Lavinsky, D.; Harris, J. S.; Palanker, D. V. *J. Neur. Eng.* **2012**, *9*, 1−22.
(10) Ghezzi, D.; Antognazza, M. R.; Dal Maschio, M.; Lanzarini, E.; Benfenati, F.; Lanzani, G. *Nat. Commun.* **2011**, *2*, 1−7.
(11) Ghezzi, D.; Antognazza, M. R.; Maccarone, R.; Bellani, S.; Lanzarini, E.; Martino, N.; Mete, M.; Pertile, G.; Bisti, S.; Lanzani, G.; Benfenati, F. *Nat. Photonics* **2013**, *7*, 400−406.
(12) Gautam, V.; Rand, D.; Hanein, Y.; Narayan, K. S. *Adv. Mater.* **2013**, *133*, 17942−17949.
(13) Lugo, K.; Miao, X. Y.; Rieke, F.; Lin, L. Y. *Biomed. Opt. Express* **2012**, *3*, 447−454.
(14) Molokanova, E.; Bartel, J. A.; Zhao, W.; Naasani, I.; Ignatius, M. J.; Treadway, J. A.; Savtchenko, A. *Biophotonics* **2008**, available from http://photonics.com/Article.aspx?AID=33995.
(15) Pappas, T. C.; Wickramanyake, W. M. S.; Jan, E.; Motamedi, M.; Brodwick, M.; Kotov, N. A. *Nano Lett.* **2007**, *7*, 513−519.
(16) Winter, J. O.; Liu, T. Y.; Korgel, B. A.; Schmidt, C. E. *Adv. Mater.* **2001**, *13*, 1673−1677.
(17) Nyberg, T.; Shimada, A.; Torimitsu, K. *J. Neurosci. Methods* **2007**, *160*, 16−25.
(18) Manceau, M.; Rivaton, A.; Gardette, J. L.; Guillerez, S.; Lemaitre, N. *Polym. Degrad. Stab.* **2009**, *94*, 898−907.
(19) Hintz, H.; Egelhaaf, H. J.; Luer, L.; Hauch, J.; Peisert, H.; Chasse, T. *Chem. Mater.* **2011**, *23*, 145−154.
(20) Deisseroth, K. *Nat. Methods* **2011**, *8*, 26−29.
(21) Bi, A. D.; Cui, J. J.; Ma, Y. P.; Olshevskaya, E.; Pu, M. L.; Dizhoor, A. M.; Pan, Z. H. *Neuron* **2006**, *50*, 23−33.
(22) Lagali, P. S.; Balya, D.; Awatramani, G. B.; Munch, T. A.; Kim, D. S.; Busskamp, V.; Cepko, C. L.; Roska, B. *Nat. Neurosci.* **2008**, *11*, 667−675.
(23) Yuan, C. T.; Wang, Y. G.; Huang, K. Y.; Chen, T. Y.; Yu, P.; Tang, J.; Sitt, A.; Banin, U.; Millo, O. *ACS Nano* **2012**, *6*, 176−182.
(24) Gabay, T.; Ben-David, M.; Kalifa, I.; Sorkin, R.; Abrams, Z. R.; Ben-Jacob, E.; Hanein, Y. *Nanotechnology* **2007**, *18*, 1−6.
(25) Shoval, A.; Adams, C.; David-Pur, M.; Shein, M.; Hanein, Y.; Sernagor, E. *Front. Neuroeng.* **2009**, *2*, 1−8.
(26) Zhang, X.; Prasad, S.; Niyogi, S.; Morgan, A.; Ozkan, M.; Ozkan, C. S. *Sens. Actuators B: Chem.* **2005**, *106*, 843−850.
(27) Sorkin, R.; Greenbaum, A.; David-Pur, M.; Anava, S.; Ayali, A.; Ben-Jacob, E.; Hanein, Y. *Nanotechnology* **2009**, *20*, 1−8.
(28) Tran, P. A.; Zhang, L. J.; Webster, T. J. *Adv. Drug Delivery Rev.* **2010**, *62*, 667−667.
(29) Voge, C. M.; Stegemann, J. P. *J. Neural Eng.* **2011**, *8*, 1−10.
(30) Bareket-Keren, L.; Hanein, Y. *Front. Neural Circuits* **2013**, *6*, 1−16.
(31) Nastase, C.; Mihaiescu, D.; Nastase, F.; Moldovan, A.; Stamatin, L. *Synth. Met.* **2004**, *147*, 133−138.
(32) Zou, L.; Vidalis, I.; Steele, D.; Michelmore, A.; Low, S. P.; Verberk, J. *J. Membr. Sci.* **2011**, *369*, 420−428.
(33) Carbone, L.; Nobile, C.; De Giorgi, M.; Sala, F. D.; Morello, G.; Pompa, P.; Hytch, M.; Snoeck, E.; Fiore, A.; Franchini, I. R.; Nadasan,

M.; Silvestre, A. F.; Chiodo, L.; Kudera, S.; Cingolani, R.; Krahne, R.; Manna, L. *Nano Lett.* **2007**, *7*, 2942−2950.
(34) Nann, T. *Chem. Commun.* **2005**, 1735−1736.
(35) Hermanson, G. T. *Bioconjugate Techniques*; Academic Press: London, UK, 1996.
(36) Eleftheriou, C. G.; Zimmermann, J.; Kjeldsen, H.; David-Pur, M., Hanein, Y.; Sernagor, E. In *Proceedings of the 8th Int. MEA meeting on substrate integrated microelectrode arrays*, Reutlingen, Germany, 2012.
(37) David-Pur, M.; Bareket-Keren, L.; Beit-Yaakov, G.; Raz-Prag, D.; Hanein, Y. *Biomed. Microdevices* **2014**, *16*, 43−53.
(38) Wong, W. T.; Sanes, J. R.; Wong, R. O. L. *J. Neurosci.* **1998**, *18*, 8839−8852.
(39) Bruhn, S. L.; Cepko, C. L. *J. Neurosci.* **1996**, *16*, 1430−1439.
(40) Mey, J.; Thanos, S. *Brain Res. Rev.* **2000**, *32*, 343−379.
(41) Verra, D. M.; Contin, M. A.; Hicks, D.; Guido, M. E. *Invest. Ophthalmol. Vis. Sci.* **2011**, *52*, 5111−5120.
(42) Neumann, T.; Ziegler, C.; Blau, A. *Brain Res.* **2008**, *1207*, 120−127.
(43) Freeman, D. K.; Rizzo, J. F.; Fried, S. I. *J. Neural Eng.* **2011**, *8*, 1−18.
(44) Sernagor, E.; Eglen, S. J.; Wong, R. O. L. *Prog. Retin. Eye Res.* **2001**, *20*, 139−174.
(45) Weaver, J. E.; Dasari, M. R.; Datar, A.; Talapatra, S.; Kohli, P. *ACS Nano* **2010**, *4*, 6883−6893.
(46) Hu, L.; Zhao, Y. L.; Ryu, K.; Zhou, C.; Stoddart, J. F.; Gruner, G. *Adv. Mater.* **2008**, *20*, 939−946.
(47) Lovric, J.; Bazzi, H. S.; Cuie, Y.; Fortin, G. R. A.; Winnik, F. M.; Maysinger, D. *J. Mol. Med.* **2005**, *83*, 377−385.
(48) Chan, W. H.; Shiao, N. H.; Lu, P. Z. *Toxicol. Lett.* **2006**, *167*, 191−200.
(49) Kotov, N. A.; Winter, J. O.; Clements, I. P.; Jan, E.; Timko, B. P.; Campidelli, S.; Pathak, S.; Mazzatenta, A.; Lieber, C. M.; Prato, M.; Bellamkonda, R. V.; Silva, G. A.; Kam, N. W. S.; Patolsky, F.; Ballerini, L. *Adv. Mater.* **2009**, *21*, 3970−4004.
(50) Derfus, A. M.; Chan, W. C. W.; Bhatia, S. N. *Nano Lett.* **2004**, *4*, 11−18.
(51) Simoni, J.; Villanueva-Meyer, J.; Simoni, G.; Moeller, J. F.; Wesson, D. E. *Artif. Organs* **2009**, *33*, 115−126.
(52) Carbone, L.; Nobile, C.; De Giorgi, M.; Sala, F. D.; Morello, G.; Pompa, P.; Hytch, M.; Snoeck, E.; Fiore, A.; Franchini, I. R.; Nadasan, M.; Silvestre, A. F.; Chiodo, L.; Kudera, S.; Cingolani, R.; Krahne, R.; Manna, L. *Nano Lett.* **2007**, *7*, 2942−2950.
(53) Yin, Y.; Alivisatos, A. P. *Nature* **2005**, *437*, 664−670.
(54) Hammerle, H.; Egert, U.; Mohr, A.; Nisch, W. *Biosens. Bioelectron.* **1994**, *9*, 691−696.